Journal of Solid State Chemistry **156,** 400–407 (2001)
doi:10.1006/jssc.2000.9013, available online at http://www.idealibrary.com on IDEAL®

Microstructural Changes Induced by Thermal Treatment of Cobalt(II) Hexacyanoferrate(III) Compound

C. W. Ng,* J. Ding,* and L. M. Gan†,‡

*Department of Materials Science, National University of Singapore, Singapore 119260; †Department of Chemistry, National University of Singapore, Singapore 119260; and ‡Institute of Materials and Research Engineering, Singapore 119260

Received May 16, 2000; in revised form October 18, 2000; accepted October 27, 2000

Molecular-based magnet cobalt–iron cyanide, $K_{0.2}Co_{1.4}[Fe(CN)_6]\cdot 7H_2O$, was prepared by coprecipitation. The powder X-ray diffraction indicates a FCC crystal structure with a unit cell constant of 10.25 Å. It has a transition temperature of 11 K. The effects of heat treatment on the microstructures as well as magnetic properties in the compound were studied. Several structures were encountered during the course of annealing from room temperature to 600°C. In the as-prepared (freeze–dried) sample, the majority of the structure was found to be Fe^{III}–CN–Co^{II}, with a minor amount of Fe^{II}–CN–Co^{III} structure. The amount of Fe^{III}–CN–Co^{II} structure decreased as a function of annealing temperature. The third structure, namely Co^{II}–CN–Fe^{III} began to show up after annealing the sample at 100°C. Total decomposition of the cyanide sample occurred at 500°C. A mixture of BCC Fe–Co and a significant amount of (25 wt%) amorphous carbon particles was found in the sample annealed at 600°C. © 2001 Academic Press

I. INTRODUCTION

One of the main challenges in molecular magnetism remain to be the search for 3D materials having bulk ferro- or ferrimagnetic behavior, such as spontaneous magnetization, a hysteresis loop with high coercivity, and a high ordering temperature. Suitable molecular precursors, such as the stable and inert hexacyanometallates, have been used to build frameworks with controlled dimensionality (1). The material being studied in this work belongs to one of the Prussian blue analogs (2), namely $K_{0.2}Co_{1.4}[Fe(CN)_6]\cdot 7H_2O$. One of the Prussian blue analogs is the bimetallic cyanide derived from Prussian blue by mixing the molecular complex $[M^{III}(CN)_6]^{3-}$, whereby M is a paramagnetic trivalent 3d-transition metal ion, with paramagnetic divalent 3d transition metal cations X^{II} (2–4). One-to-one $K_xX^{II}_y[M^{III}(CN)^-_6]^{3-}_2\cdot nH_2O$ or two-to-three $X^{II}_3[M^{III}(CN)^-_6]^{3-}_2\cdot nH_2O$ stoichiometry may be obtained depending on the nature of the countercation of the hexacyanometallate(III) precursor. The driving force behind such fundamental researchs is the need for light-weight as well as high-density storage materials: the molecular level is indeed the ultimate step for storage capacity. Recently, interesting magnetic phenomena such as photoinduced magnetization has been reported for $K_{0.2}Co_{1.4}[Fe(CN)_6]\cdot 7H_2O$ (5). Moreover, some of unsolved technological problems may find its solution in these accessible polyfunctional materials. So far, the effects of thermal annealing on the magnetic cyanides have not been paid much attention. In this research work, this aspect will be studied in depth in order to probe into the microstructural changes involved in the compound during annealing.

II. EXPERIMENTAL METHODS

Cobalt(II) hexacyanoferrate(III) (Co–Fe cyanide) was obtained by mild chemistry at room temperature. The molecular complex $K^+_3[Fe^{III}(CN)_6]^{3-}$ (0.43 M) is coprecipitated with aqueous solution $Co^{II}Cl_2$ (0.83 M) at constant mechanical stirring overnight under nitrogen atmosphere. The magenta-colored precipitate was washed with distilled water and then centrifuged. The process was repeated several times until the unreacted chemicals were gone. The powder after freeze–drying appeared to be dark magenta in color. Chemical microanalysis yielded the formula of $K_{0.2}Co_{1.4}[Fe(CN)_6]\cdot 7H_2O$. This coprecipitated molecular compound was annealed in argon atmosphere at several temperatures for 2 h in order to study the possible effect of annealing on its microstructural and magnetic properties.

Thermogravimetric analysis (DuPont TGA 2950) and differential scanning calorimetry (DuPont DSC 2910), powder X-ray diffraction (Siemens XRD 5500) using Cu$K\alpha_1$ radiation, and Fourier-transform infrared spectroscopy (Bio-Rad FTS 135) were used to characterize the physical and chemical properties of the materials. The magnetic properties were investigated using vibrating sample magnetometry (Oxford 90 kOe VSM) as well as Mössbauer spectroscopy (Ranger Scientific MS 1200) in the temperature range of 4 K to room temperature. Chemical analyses

0022-4596/01 $35.00

were also conducted on all samples to confirm their chemical formulae.

III. RESULTS AND DISCUSSION

A. Powder X-Ray Diffraction (XRD)

From the XRD diffractogram of $K_{0.2}Co_{1.4}[Fe(CN)_6]\cdot 7H_2O$ as shown in Fig. 1, this compound possessed the face-centered cubic (FCC) crystal structure (3, 4) as shown in Fig. 2. In the presence of K^+ ions, a cubic framework arises. The metallic ions are arranged in a rock salt structure. Potassium ions are present in half of the tetrahedral sites of the structure and seven water molecules are present per formula unit which were assumed to be near the K^+ ions. The lattice parameter was measured to be 10.25 Å after freeze–drying, but was decreasing gradually after being subject to heat treatments. It reached 9.92 Å after being annealed at 200°C. This indicated that some microstructural changes were involved. We noticed from Fig. 1 that the FCC structure of the Co–Fe cyanide was maintained up to 250°C. Beyond 300°C, the compound began to decompose since the structure shown appeared diffused (FCC structure is distorted). Annealing at 600°C converted the cyanide into body-centered cubic (BCC) Fe–Co.

B. Thermogravimetric Analysis (TGA) and Differential Scanning Calorimetry (DSC)

Figure 3 shows the TGA and DSC measurements of the coprecipitation-derived Co–Fe cyanides, from 30 to 600°C in an inert nitrogen atmosphere at a heating rate of 10°C/min. In TGA, each slope (step) infers a loss of weight of the compound within a different temperature range, whereas in DSC, the endothermic curves (concave curves) below

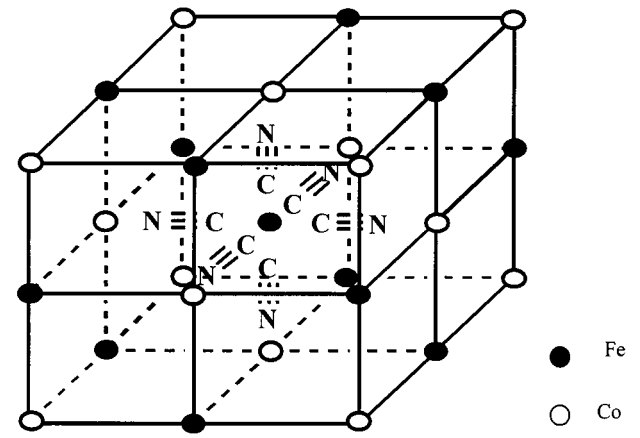

FIG. 2. The FCC structure of $K_{0.2}Co_{1.4}[Fe(CN)_6]\cdot 7H_2O$. For simplicity and clarity, the K^+ ions and coordination water molecules have been omitted. The solid and dotted lines represent the cyanide (CN^-) bonds. In an ideal cubic structure, each Fe ion is bonded to a carbon atom while each Co ion is bonded to a nitrogen atom.

200°C in the DSC indicate loss of water molecules. The exothermic curves (convex curves) correspond to the decomposition processes. Hence, the initial two steps in TGA correspond to water loss processes. From 30 to 75°C, one water molecule was lost. From 75°C onward up to 150°C, the dehydration rate increased significantly (observed from the gradient of the slope) and four water molecules were lost. From 250 to 360°C, two more water molecules were lost and partial decomposition of the cyanide began beyond that. Total decomposition occurred at around 500°C. Indeed, the sample annealed at 600°C consisted of a majority of Fe–Co particles and a significant amount of amorphous carbon

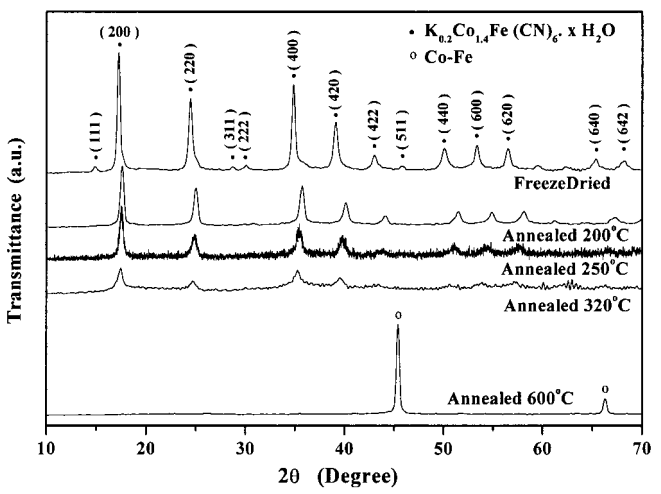

FIG. 1. The XRD diffractogram of $K_{0.2}Co_{1.4}[Fe(CN)_6]\cdot 7H_2O$ and its derivatives.

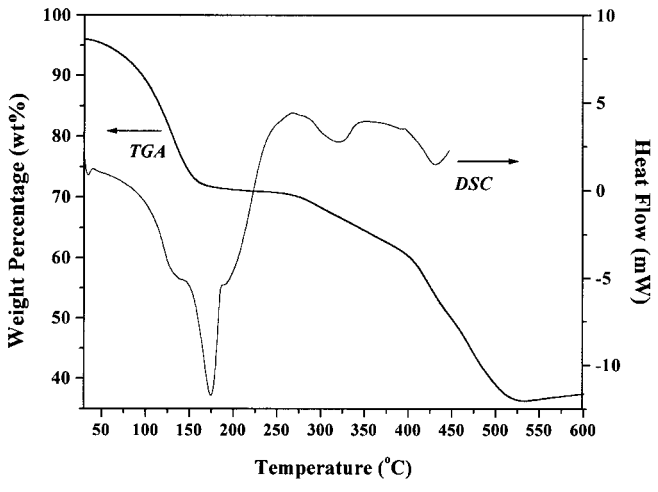

FIG. 3. Thermogravimetric analysis (TGA) and differential scanning calorimetry (DSC) spectrum of freeze–dried Co–Fe cyanide, $K_{0.2}Co_{1.4}[Fe(CN)_6]\cdot 7H_2O$.

particles (~20 wt%), and virtually no nitrogen as determined by the chemical microanalysis.

C. Fourier-Transform Infrared (FTIR)

The vibrational spectra of cyano complexes have been studied previously (6, 7). Cyano complexes are easily identified since they exhibit sharp band stretching, ν(CN), at 2200–2000 cm^{-1}. Free CN^{-1} has ν(CN) of about 2060 cm^{-1} in aqueous solution. When complexing with metals, CN^{-} ion tends to act as a σ donor by donating electrons to the metal. σ Donation tends to raise the ν(CN) since electrons are removed from the 5σ orbital, which is weakly antibonding. The ν(CN) of cyano complex is governed by the electronegativity, the oxidation state, and the coordination number of the metal bonded directly to the cyanide bond. Comparing $\nu(Fe^{III}–CN–Co^{II})$ and $\nu(Fe^{II}–CN–Co^{III})$, the previous band should have a higher wavenumber (frequency) than the latter due to the higher oxidation number of Fe ion and hence a stronger σ-bonding. In fact, measurement results (Fig. 4) showed two major peaks at 2158 and 2118 cm^{-1} for $K_{0.2}Co_{1.4}[Fe(CN)_6]\cdot 7H_2O$, which could be assigned to $\nu(Fe^{III}–CN–Co^{II})$ and $\nu(Fe^{II}–CN–Co^{III})$, respectively (6). Another major peak appeared at 2072 cm^{-1}. This peak was deduced to be the $\nu(Co^{II}–CN–Fe^{III})$. This is due to the higher electronegativity of Co^{II} ions compared to Fe^{II} ions (6). Therefore the σ donation in this case will be less, and the value of $\nu(Co^{II}–CN–Fe^{III})$ is expected to be lower than that of $\nu(Fe^{II}–CN–Co^{III})$. In all the different structures discussed above, the metal ions are assumed to be sixly coordinated to the CN^{-1} ions.

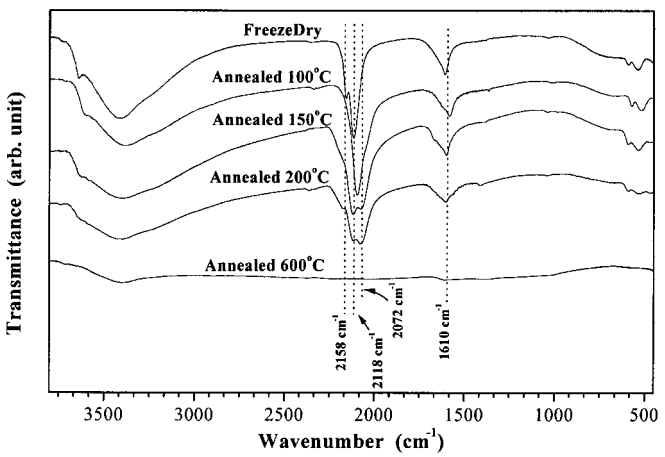

FIG. 4. The Fourier-transform infrared (FTIR) spectrum of Co–Fe cyanide treated at various temperatures. The peaks indicated at 2158, 2118, and 2072 cm^{-1} correspond to the CN stretching in $Fe^{III}–CN–Co^{II}$ structure, $Fe^{II}–CN–Co^{III}$ structure, and $Co^{II}–CN–Fe^{III}$ structure respectively. O–H bending was observed at 1610 cm^{-1}. Sample annealed at 600°C was decomposed totally to Fe–Co particles and thus showed no CN stretching band.

Other than the three major vibrational bands mentioned above, less significant vibrational bands on the lower frequency range were also observed. This includes the band stretching, $\nu(Fe^{II}–C)$ at 590 cm^{-1} and $\nu(Fe^{III}–C)$ at 532 cm^{-1}, as well as the band bending, $\delta(Fe^{II}–CN)$ at 424 cm^{-1} and $\delta(Fe^{III}–CN)$ at 387 cm^{-1}. The band at 1610 cm^{-1} coresponds to the ν(O–H) of the lattice water molecules.

Initially, only two cyano stretching bands were present (Fig. 4), corresponding to the $Fe^{III}–CN–Co^{II}$ structure (2158 cm^{-1}) and $Fe^{II}–CN–Co^{III}$ structure (2118 cm^{-1}). As annealing temperature is increased, the structure $Co^{II}–CN–Fe^{III}$ (2072 cm^{-1}) began to show up. The band corresponding to the last structure was steadily increasing in intensity and most prominently observed in sample annealed at 200°C. On the other hand, the band corresponding to the $Fe^{III}–CN–Co^{II}$ structure was diminishing in intensity (quantity) while that of $Fe^{III}–CN–Co^{II}$ structure was always present with noticeable intensity. It is clear that the effect of annealing on the Co–Fe cyanide is to swap the position of Fe^{III} ions and that of the Co^{II} ions around the octahedrally symmetrical coordination of CN^{-1} ligands. The structure $Fe^{III}–CN–Co^{II}$, nevertheless, is always present after the cyanide was subject to annealing and is gaining in intensity with annealing temperature.

For sample annealed at 600°C, total decomposition of the cyanide into the BCC Fe–Co particles and thus no cyanide band stretching was observed.

D. Mössbauer Spectroscopy

As expected, the magnetic properties of these Co–Fe cyanides (whether heat-treated or not) are influenced directly by the symmetry of the cubic crystal field. This aspect was probed in detail by using the ^{57}Fe Mössbauer spectroscopy. The FTIR spectrum shown earlier gave the several structures involving different iron valencies and positions, but only qualitatively. The Mössbauer spectrum, on the other hand, gave the quantitative results.

The ambient temperature ^{57}Fe Mössbauer spectra of Co–Fe cyanides (8) annealed at different temperatures were shown in Fig. 5. Two doublets and one singlet were encountered. A small amount (11%) of singlet with chemical shift (CS) of -0.07 mm/s and majority (89%) doublet with CS of -0.15 mm/s and quadrupole splitting (QS) of 0.384 mm/s were observed in the as-prepared (freeze–dried) sample. If the sample was annealed at 100°C, the singlet increased in amount and in addition to the first doublet, a second doublet (CS = 0.19 mm/s and QS = 1.01 mm/s) appeared, but at a more positive CS. As annealing temperature was getting higher, the amount of the singlet and the second doublet increased relatively to the first doublet. Comparing these results to those of the FTIR, it is clear that the singlet can be assigned to the structure $Fe^{II}–CN–Co^{III}$, the first doublet (CS = -0.07 mm/s) assigned to the structure $Fe^{III}–CN–$

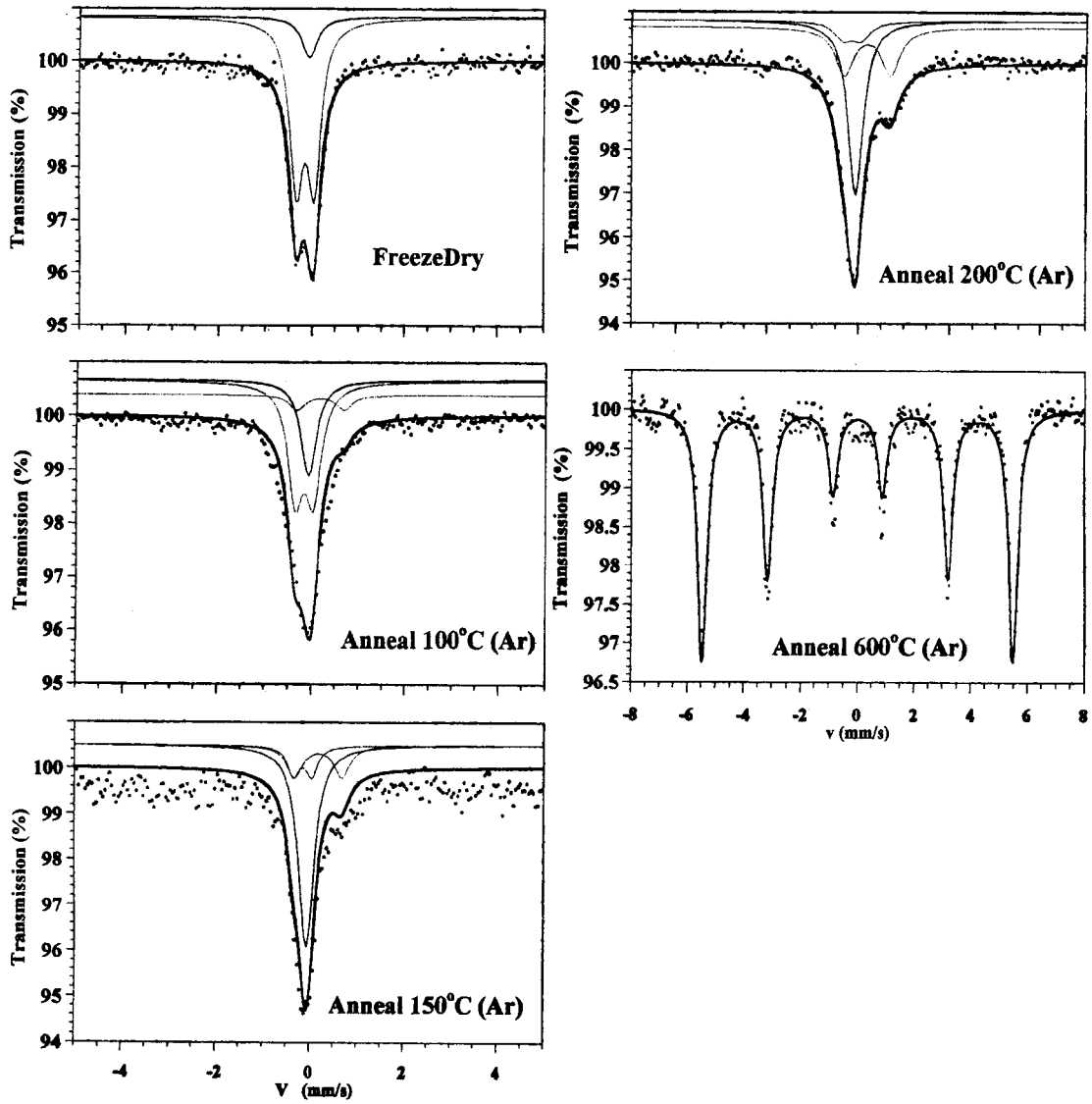

FIG. 5. Ambient temperature (290K) ^{57}Fe Mössbauer spectra of Co–Fe cyanides annealed at different temperatures.

Co^{II} and the second doublet (CS = 0.19 mm/s) assigned to the structure Co^{II}–CN–Fe^{III}. The singlet arose because the low-spin Fe^{II} ($S = 0$) ion is situated in a symmetrical octahedral CN ligand coordination sphere. No electrical field gradient (EFG) exist and hence no quadrupole splitting (9–11). Whereas for low spin Fe^{III} ($S = \frac{1}{2}$) ion, due to the half-spin on the cation, the valence electron contribution to the EFG is nonzero, so a doublet is observed. In Mössbauer spectroscopy, the chemical shift (CS) arises because the electron density at the nucleus (*s*-orbital electron or *s*-electron for short) interacts with the positive nuclear charge (9–11). In a complex, the valence electron from the partially filled valence orbitals which contribute to the *s*-electron density at the nucleus is very sensitively affected by changes in the electronic structure of the valence shell by the surrounding chemical environments, such as change of oxidation state, of spin state, of bond properties by electron delocalization, etc. For ^{57}Fe, it has been shown that increasing *s*-electron density at the nucleus produces a negative shift in the value of CS. The *s*-electron density in Fe^{III} ions will be dependent on the extent of the shielding by the 3d valence electrons. Comparing C (carbon atom) and N (nitrogen atom), N is more electronegative than C. Therefore when Fe^{III} ion is bonded to C atom, as in the structure Fe^{III}–CN–Co^{II}, the shielding of the *s*-electron would be less effective since lower 3d electron density would be found on Fe^{III} ion (i.e., 3d electrons tend to "flow over" to the C atom). This causes a stronger attraction of the electron cloud by the nuclear charge and thus increases the nuclear electronic charge density (9–11). On the other hand, when Fe^{III} ion is

TABLE 1
Illustration of the Chemical Shift (CS), Quadrupole Splitting (QS), and Hyperfine Field (HF) of the Different Structures during Different Stages of Thermal Treatment

	Temperature: 290 K		
Structure	CS (mm/s)	QS (mm/s)	HF (mm/s)
Fe^{III}–CN–Co^{II}	− 0.15	0.38	—
Fe^{II}–CN–Co^{III}	− 0.07	—	—
Co^{II}–CN–Fe^{III}	0.19	1.01	—
FCC Fe–Co	0.01	− 0.004	33.96

bonded to N atom, as in the structure Co^{II}–CN–Fe^{III}, the shielding of the *s*-electron would be more effective as higher 3d electron density would be found on Fe^{III} ion and thus lower *s*-electron density at the ^{57}Fe nucleus. This in turn gives rise to a more positive CS.

When Fe^{III} ion is bonded to the N atoms, it will be in a less cubic symmetry than when it is bonded to the carbon atoms due to the nonstoichiometric formula of $K_{0.2}Co_{1.4}[Fe(CN)_6]\cdot nH_2O$ since some of the N atoms will be bonded to the oxygen atoms from lattice water molecules (12). The extra lattice contribution to the EFG in this case results in the greater value of quadrupole splitting (QS) of the structure Co^{II}–CN–Fe^{III} (QS = 1.01 mm/s) compared to the structure Fe^{III}–CN–Co^{II} (QS = 0.38 mm/s).

The various Mössbauer parameters corresponding to the different structures encountered in Co–Fe cyanides, measured at 290 K, are tabulated in Table 1 and their relative amounts found in the cyanides annealed at different temperatures are tabulated in Table 2. These results are consistent with the FTIR measurements (Fig. 4). In the freeze–dried sample, the majority of the structure is Fe^{III}–CN–Co^{II} (first doublet) and a small amount of Fe^{II}–CN–Co^{III} (singlet). In FTIR, both the bands (2158 and 2118 cm^{-1}) corresponding to these two structures were observed. The structure Co^{II}–CN–Fe^{III} (second doublet) began to show up as the annealing reached 100°C. This was shown as a shoulder at 2118 cm^{-1} in the FTIR, and became more prominent as annealing temperatures got higher. Meanwhile, the amount of the Fe^{III}–CN–Co^{II} decreased relatively to that of Co^{II}–CN–Fe^{III} and became insignificant ($\sim$ 10%) at 200°C as observed in the Mössbauer. The same phenomenon was also observed in FTIR. The peak corresponding to the Fe^{III}–CN–Co^{II} at 2158 cm^{-1} almost disappeared while that of Co^{II}–CN–Fe^{III} gained in intensity at 200°C.

From the Mössbauer spectra of the freeze-dried Co–Fe cyanide taken at 4 K, the doublet corresponding to the structure Fe^{III}–CN–Co^{II} collapsed into a sextet below its Curie temperature of 11 K. The singlet corresponding to the structure Fe^{II}–CN–Co^{III} remained as it is even at cryogenic temperature. This is due to the fact that Fe^{III} ion (low–spin) is a spin carrier with $S = \frac{1}{2}$ while Fe^{II} ion (low–spin) is diamagnetic with no spin.

In a nutshell, the effect of annealing on the Co–Fe cyanide is to change the microstructures of the compound from the initial majority structure Fe^{III}–CN–Co^{II} to the structures Fe^{II}–CN–Co^{III} and Fe^{III}–CN–Co^{II}.

As the sample was annealed at 600°C, the cyanide phase was totally decomposed into the BCC Fe–Co particles as discussed in the TGA and DSC session. A sextet, arising from the magnetic Fe–Co particles, was expected from the Mössbauer spectra at ambient temperature.

E. Vibrating Sample Magnetometry (VSM)

Assuming magnetic quenching of the 3d orbitals in the transition metals, the theoretical value of μ for each magnetic center can be derived as

$$\mu_{(\mathrm{Fe\,or\,Co})} = g\mu_B\,[S_{(\mathrm{Fe\,or\,Co})}(S_{(\mathrm{Fe\,or\,Co})} + 1)]^{\frac{1}{2}}, \qquad [1]$$

TABLE 2
Quantities of the Various Structures Present in the Fe–Co Cyanides under Different Thermal Treatments Measured by ^{57}Fe Mössbauer at 290 K

	Structures			
Thermal treatment	Fe^{III}–CN–Co^{II}	Fe^{II}–CN–Co^{III}	Co^{II}–CN–Fe^{III}	FCC Fe–Co
Freeze–dried	89.0	11.0	—	—
Annealed 100°C (in argon)	63.0	28.0	9.0	—
Annealed 150°C (in argon)	14.6	65.1	20.3	—
Annealed 200°C (in argon)	12.3	52.9	34.7	—
Annealed 600°C (in argon)	—	—	—	100.0

where g is the gyromagnetic factor which has been taken to be 2 and S is the total spin. So, for a single moiety such as $K_{0.2}Co_{1.4}[Fe(CN)_6]\cdot 7H_2O$, the total magnetic moment per chemical formula is given by $\mu_{T,Theo} = \mu_{Fe} + 1.4\,\mu_{Co}$. Finally the theoretical molar saturation magnetization per unit formula is $M_{s,Theo} = N\mu_T$ (in the unit of emu/mol) = $N\mu_T$/relative molecular mass (in the unit of emu/g), where N denotes the Avogadro's number (6.023×10^{23} mol^{-1}).

At sufficiently low field, χ_p, the magnetic susceptibility for paramagnetic material is shown to be

$$\chi_p = N^2\mu_T^2/(3RT). \qquad [2]$$

This is known as the Curie law. R denotes the universal gas constant (8.3×10^7 erg/G mol^{-1} K^{-1}) and T the absolute temperature.

On the other hand, the magnetic susceptibility for ferromagnetic material, χ_f, for temperature range above its Curie–Weiss temperature (T_c), can be obtained from the Curie–Weiss law as shown:

$$\chi_f = N^2\mu_T^2/[3R(T - T_c)] \qquad [3]$$

By plotting the value of χ_f (taken from the experimental value of magnetization, M, against magnetic field, H) versus T, T_c can be obtained. Once the T_c value is known, the magnetic moment per unit formula, μ_T, in each compound can be determined from Eq. [3].

Preliminary magnetization curves of the freeze–dried sample are shown in Fig. 6a. In this complex compound, both the ferromagnetic transition metal ions Fe and Co form an ordered three-dimensional ferrimagnetic network with CN^- groups as bridging ligands. From the Curie–Weiss law, the transition temperature T_c, was estimated to be 11 ± 2 K (Fig. 7a), which is very close to those reported for Co–Fe cyanide (3, 13). Hard magnetic properties were observed in the hysteresis loops taken below the Curie-Weiss temperature. As reported previously, the coercivity was expected to be in the range of 0.7–0.9 kOe at liquid helium temperature (3). The coercivity measured at 4 K was 1.5 kOe with a remanance of 8.2 emu/g in this experiment. This high value of coercivity was due to the pure phase synthesized as well as ultrafine Fe–Co particles.

Figure 6b showed the temperature-dependent magnetization curves for cyanide sample annealed at 150°C. The sample showed no hysteresis and remained paramagnetic throughout the whole temperature range from room temperature down to 4 K (Fig. 7b).

A summary of the magnetic parameters T_c, μ_{Fe}, μ_{Co}, $\mu_{T,Theo}$, and $\mu_{T,Exp}$ for Co–Fe cyanides treated at different temperatures is tabulated in Table 3. The experimental value of μ_T can also be derived from the experimental saturation magnetization $M_{s,Exp}$. The value of $M_{s,Exp}$ was

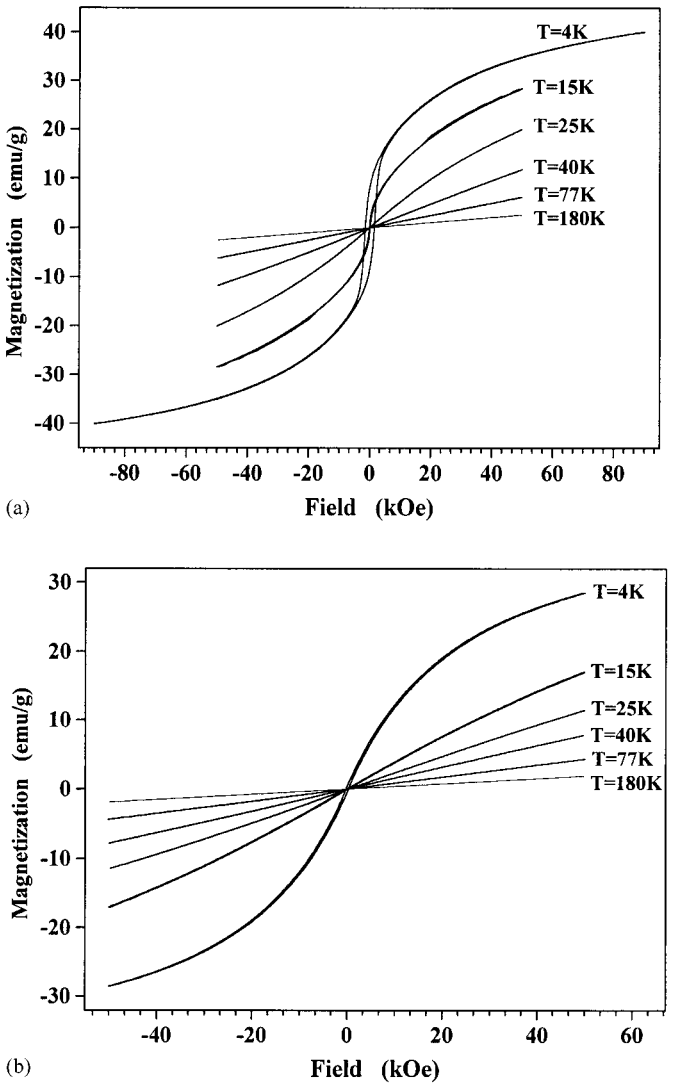

FIG. 6. The magnetization curves measured by VSM as a function of temperature for (a) freeze–dried sample and (b) sample annealed at 150°C.

derived from the extrapolation of M value in the plot of M versus $1/H$ with magnetic field (H) extended to infinity, using the magnetization curve measured at 4 K.

Assuming that Fe^{III} and Co^{II} ions are arranged ferrimagnetically, using the theoretical value of magnetic moment, $\mu_{T,Theo} = 3.7\,\mu_B$ (from Table 3), we obtained $M_{s,Theo} = 48.1$ emu/g considering a density of 2.26 g/cm^3 of the freeze–dried sample, $K_{0.2}Co_{1.4}[Fe(CN)_6]\cdot 7H_2O$ (relative molecular mass = 428.41 g/mol). This result fitted well the experimental result of saturation magnetization, $M_{s,Exp.} = 47.8$ emu/g, confirming the ferrimagnetism of the Fe^{III}–CN–Co^{II} structure.

For the cyanide calcined at 150°C in argon, having the chemical formula of $K_{0.2}Co_{1.4}[Fe(CN)_6]\cdot 7H_2O$ (relative molecular mass = 356.41 g/mol), there is 65% of the

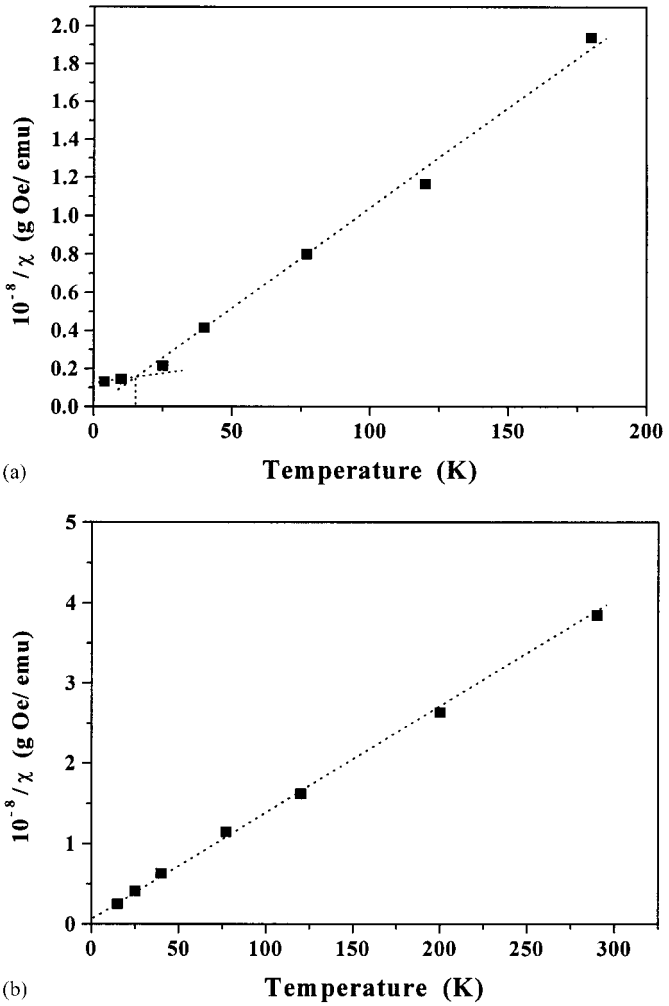

FIG. 7. Temperature dependence of $1/\chi$ for samples: (a) freeze–dried; (b) annealed 150°C in argon. Sample (a) has a transition temperature at 11 K, while sample (b) at below 4 K. Notice the abrupt transition at 11 K in sample (a). Transition temperature signifies the change from paramagnetism to ferromagnetism. $1/\chi$ was obtained from the ratio of magnetization, M (emu/g), to magnetic field, H (Oe).

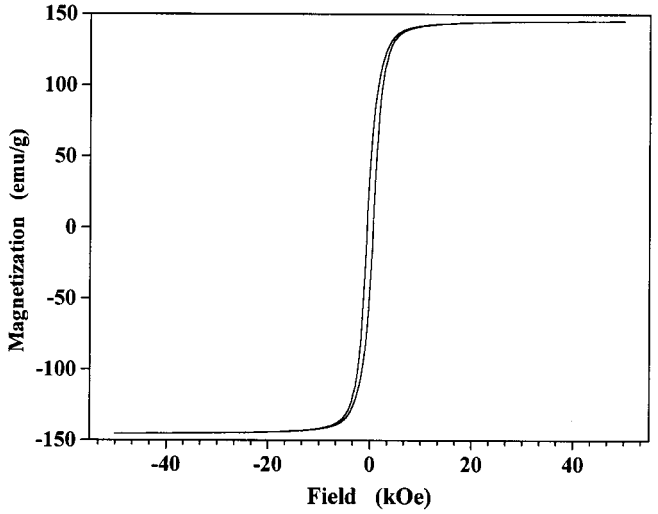

FIG. 8. Magnetization curve of Co–Fe cyanide annealed at 600°C, which consists mainly of Fe–Co particle and 25 wt% amorphous carbon particles. M_s values as high as 146 emu/g with a coercivity of 0.6 kOe were observed.

Fe^{II}–CN–Co^{III} structure together with 15% of the Fe^{III}–CN–Co^{II} structure and 20% Co^{II}–CN–Fe^{III} structure as determined from the Mössbauer spectroscopy. Taking into account the individual percentage contribution to the total magnetic moment of these structures, the theoretical value would be around 4.5 μ_B (Table 3), assuming parallel (ferromagnetic) coupling of the Co^{III} ions in the Fe^{II}–CN–Co^{III} structure (Fe^{II} ion is diamagnetic since it carries no net spin). The experimental result fitted with the Curie law and that obtained from the $M_{s,Exp}$ value yielded $\mu_{T,Exp} = 4.1\ \mu_B$ and 3.1 μ_B, respectively. The Langevin function fitting of the magnetization curve at 4 K also gave $\mu_{T,Exp} = 3.3\ \mu_B$. The above results suggest that the Co^{III} ions are arranged ferrimagnetically within the cyanide compound annealed at 150°C. Similar magnetic properties were also observed in sample annealed at 200°C.

In the sample annealed at 600°C, consisting of BCC Fe–Co particles, a saturation magnetization of 146 emu/g with a coercivity of 0.6 kOe was determined from the VSM at 290 K (Fig. 8). The transmission electron micrograph of the sample was shown in Fig. 9. An oxide layer was probably formed on the surface of the particle.

TABLE 3

Summary of the Curie–Weiss Temperature (T_c), Theoretical Magnetic Moment per Fe(Co) Ion ($\mu_{Fe(Ni)}$), Theoretical Magnetic Moment ($\mu_{T,Theo}$), and Experimental Magnetic moment (obtained by: (1) fitting with Curie or Curie–Weiss Law ($\mu_{T,Expl}$); (2) fitting with $M_{s,Exp} = N\mu_T$/molecular mass ($\mu_{T,Exp2}$)) of the Majority Structures at Different Stages of Annealing

Majority structure	Treatment	T_c (K)	μ_{Fe} (μ_B)	μ_{Co} (μ_B)	$\mu_{T,Theo}$ (μ_B)	$\mu_{T,Expl}$ (μ_B)	$\mu_{T,Exp2}$ (μ_B)
Fe^{III}–CN–Co^{II}	Freeze–dried	11	1.7	3.9	3.7	4.5	3.7
Fe^{II}–CN–Co^{III}	Annealed 150°C in argon	—	0	4.9	4.5	4.1	3.2

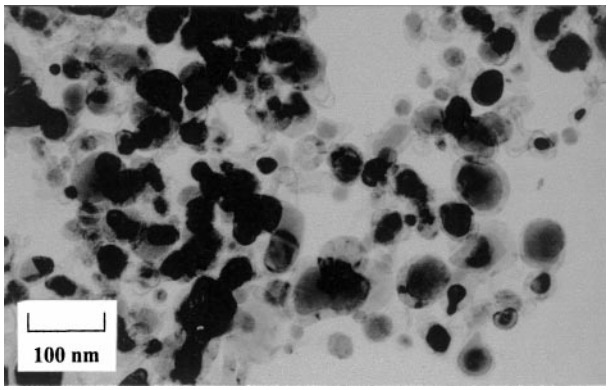

FIG. 9. Transmission electron micrograph of BCC Fe–Co particles formed after annealing Co-Fe cyanide at 600°C. Formation of an oxide layer was observed on the surface of the particle.

IV. CONCLUSION

The low-temperature molecular magnet iron–cobalt cyanide powder was prepared by coprecipitation method where the particle size is in the nanoscale range. It possessed an FCC crystal structure with lattice parameter of around 10 Å. This ferrimagnetic powder has a transition temperature of 11 K. The effects of annealing on its physical as well as magnetic properties were studied. The Fe^{III}–CN–Co^{II} structure is the major structure in the freeze–dried Co–Fe cyanide. As the cyanide was annealed at higher temperatures, two other structures appeared, namely Fe^{II}–CN–Co^{III} and Co^{II}–CN–Fe^{III} as probed by FTIR and Mössbauer techniques. After annealing at 150°C, Fe^{II}–CN–Co^{III} appeared to be the major structure. Due to the ferrimagnetic nature of the Co^{III} ions and diamagnetic Fe^{II} ions, this structure has a lower total magnetic moment, leading to a lower saturation magnetization compared to the major structure Fe^{III}–CN–Co^{II} in the freeze–dried sample. Complete decomposition of the cyanide phase occurred at around 500^0C, whereby nanoscale BCC Fe–Co particles were found, as a well as a significant amount of amorphous carbon particles. These soft magnetic Fe–Co particles have a M_s value as high as 146 emu/g and coercivity of 0.6 kOe.

REFERENCES

1. P. M. Allemand, K. C. Khemani, A. Koch, K. Holczer, S. Donovan, G. Grüder, and J. D. Thomson, *Science* **25,** 301 (1991).
2. D. Gatteschi, O. Kahn, J. S. Miller, F. Palacio (Eds.), "Molecular Magnetic Materials," NATO ASI Series E: Applied Science, Vol. 198, 1991.
3. S. Juszczyk, C. Johansson, M. Hanson, A. Ratuszna, and G. Malecki, *J. Appl. Phys.: Condens. Matter* **6,** 5697 (1994).
4. A. Ratuszna, S. Juszczyk, and G. Malecki, *Powder Diffraction* **10,** 300 (1995).
5. O. Sata, T. Iyoda, A. Fujishima, and K. Hashimoto, *Science* **272,** 704 (1996).
6. K. Nakamoto (Ed.), "Infrared and Raman Spectra of Inorganic and Coordination Compounds. Part B: Applications in Coordination, Organometallic and Bioorhganic Chemistry," 5th ed. Wiley Interscience, New York, 1997.
7. K. Chandra, Deo Raj, and S. P. Puri, *J. Chem. Phys.* **46,** 1466 (1967).
8. David B. Brown and D. F. Shriver, *Inorg. Chem.* **8,** 37 (1969).
9. P. Gütlich, R. Link, and A. Trautwein (Eds.), "Mössbauer Spectroscopy and Transition Metal Chemistry." Springer-Verlag, New York, 1978.
10. R. S. Drago (Ed.), "Physical Methods In Inorganic Chemistry." Reinhold Pub. Corp., New York, 1965.
11. N. N. Greenwood and T. C. Gibb (Eds.), "Mössbauer Spectroscopy," Chapman & Hall, London, 1971.
12. Andreas Ludi and Hans Ulrich Güdel, *Struct. Bonding* **14** (1973).
13. O. Kahn, *in* "Molecular Magnetism: From Molecular Assemblies to the Devices," (E. Coronado, P. Delhaés, D. Gatteschi, and J. S. Miller, Eds.), NATO ASI Series E: Applied Science, Vol. 321, pp. 243, VCH, Weinheim/New York (1993).